Lipid lateral self-diffusion drop at liquid-gel phase transition

Boris Kheyfets,[1,*] Timur Galimzyanov,[2,†] and Sergei Mukhin[1]
[1]*National University of Science and Technology MISIS, Moscow, Russia*
[2]*A. N. Frumkin Institute of Physical Chemistry and Electrochemistry RAS, Moscow, Russia*

(Received 27 November 2018; published 16 January 2019)

A drop of lipid lateral self-diffusion coefficient at the liquid-gel phase transition in lipid membranes is calculated. So far this drop was missing theoretical description. Our microscopic model captures so-called subdiffusion regime, which takes place on 1 ps–100 ns timescale and reveals a jump of self-diffusion coefficient. Calculation of the jump is based on our recent study of liquid-gel phase transition. Subdiffusive regime is described within the free volume theory. Calculated values of self-diffusion coefficient are in agreement with quasielastic neutron scattering measurements. Self-diffusion coefficient is found to be composed of two factors: one is related to an area per lipid change at the phase transition, and the other one is due to an order of magnitude change in the stiffness of entropic repulsive potential.

DOI: 10.1103/PhysRevE.99.012414

I. INTRODUCTION

Cells of living organisms are well separated from each other. One of the main barriers separating cells from environment is lipid membrane. For decades lipid membrane was considered just as a platform for proteins, with all biological functions, such as signaling or transport, attributed to proteins alone [1]. This point of view started to change as a number of studies showed the influence of lipid environment exercises on the protein functioning [2–5]. These observations cause an ongoing increase of interest to the lipid membrane.

Cell membrane consists of more than the hundred different types of lipids [6,7]. This makes cell membrane a complex multicomponent system which is difficult to investigate *in situ*. One of the popular approaches to understand its thermodynamic properties is analyzing the model systems, consisting of limited and controlled amounts of components. The simplest one is a single-component lipid membrane.

Lipid membrane is a two-dimensional liquid crystal. At lower temperatures it undergoes a first-order phase transition to a gel phase, so-called main phase transition [8]. More precisely, depending on the lipid type, the membrane can undergo a number of phase transitions in the vicinity of the main phase transition. These intermediate phases may include the ripple phase [9,10] and interdigidated gel phase [11]. At least some of these phases need a certain symmetry breaking at the phase transition. We will limit our model to merely two main phases liquid and gel ones, and assume that all possible intermediate transitions are uncoupled and do not affect the main phase transition. We also assume that there is no symmetry breaking at the main phase transition.

For most lipids a corresponding single-component lipid membrane undergoes this transition at a temperatures significantly lower than the room temperature, with an exception of lipids with a saturated hydrophobic chains, such as DMPC ($T_m = 24^\circ$C) and DPPC ($T_m = 41^\circ$C). A number of studies also suggest that cholesterol might induce gel phase in lipid membrane [12,13].

One of the important dynamic properties of the lipid membrane is the lateral self-diffusion coefficient. With diffusion being the main mechanism of lateral movement of the membrane components the value of self-diffusion coefficient influences cell phenomena involving protein rearrangements, such as fusion [14,15] and fission [16,17]. Microscopic picture of diffusion and its behavior at the main phase transition is still actively debated in the literature [18–22]. At the main phase transition the value of self-diffusion coefficient jumps by several times. Despite the wide interest attracted by the lipid self-diffusion this change of self-diffusion coefficient at the liquid-gel phase transition is still lacking theoretical description.

There are a number of ways to measure the self-diffusion coefficient in lipid bilayers: neutron scattering [23–25], inelastic x-ray scattering [26], NMR [18], fluorescence recovery after photobleaching [27], and many others. The general conclusion is that the self-diffusion coefficient obtained by methods operating on a nanosecond time scale is two orders of magnitude lower then one provided by the methods measuring it on a microsecond time scale [28].

This discrepancy has been explained within free volume theory [29] by varying effectiveness of diffusion events: only some jump events at the nanosecond scale contribute to diffusion on a microsecond scale due to lipids jumping forward and backward [28]. The greater number of jumps on the nanosecond timescale led to a regime named "rattling in a cage". During the past decade a number of molecular dynamics studies probed the microscopic picture, and found that self-diffusion on a nanosecond timescale appears to be driven by collective movements of nanoclusters of about five lipid molecules [30,31] rather than jumps of individual lipids. However, a new generation of quasi-elastic neutron scattering (QENS) study allowed to study self-diffusion in

*kheyfboris@misis.ru
†Also at National University of Science and Technology MISIS.

lipid bilayers with picosecond resolution and the conclusion is that lipids move independently [32], but due to a steric hindrance this motion causes a rearrangement of the nearest neighbor molecules, thus providing a picture compatible with diffusion of loosely bound dynamic nanoclusters.

Thus, lipid self-diffusion on a nanosecond time scale is a good fit for single-molecule mean-field approaches. One of the approaches to a lipid diffusion is a free-volume theory, mentioned above. According to this theory [20,29], the diffusion coefficient D is averaged over the distribution $P(A_v)$ of the nearby void area formed by membrane dynamical defects, accessible for the chain: $D = \int_{A_n}^{\infty} D(A_v)\, P(A_v)\, \mathrm{d}A_v$, where $D(A_v)$ is a diffusion constant inside the accessible area A_v, and A_n is minimal accessible area necessary for a chain's rattling (Brownian movement).

The value of the lipid self-diffusion coefficient should not be confused with the value of diffusion coefficient of membrane inclusions, such proteins or lipid rafts. Diffusion of inclusions in a lipid membrane is a completely different phenomenon, with a larger characteristic length scale, and hence described via continuous hydrodynamics based approaches. See, e.g., [33] for a recent review.

In this paper we apply a microscopic flexible strings model of a lipid in an entropic repulsive mean-field to a free-volume approach, augmented with an activation energy contribution [34]. Thus, the jump of a lipid into the nearby void from the cage A_v depends on two independent events: availability of the large enough cage area A_v for the lipid to rattle, $P(A_v)$, and an activation energy E for the lipid to jump $P(E)$:

$$D = \int_{A_n}^{\infty} \int_{E_a}^{\infty} D(A_v) \cdot P(A_v) \cdot P(E)\, \mathrm{d}E\, \mathrm{d}A_v. \qquad (1)$$

Here, E_a is a minimal energy required for the jump into the void.

This paper is organized as follows. In Sec. II we briefly recap the flexible strings model [35,36] as well as its application to the description of liquid-gel phase transition. In Sec. III we use the model to calculate lipid self-diffusion coefficient using Eq. (1) of lipid membrane above and below the main phase transition temperature and compare with experimental data. Section IV contains a discussion of obtained results and clarification of the physical mechanism underlying the self-diffusion drop and conclusions.

II. CALCULATION

A. Flexible strings model

Flexible strings model is treated within a mean-field theory, that considers a lipid in a self-consistent field of other lipids in the same monolayer. Layers of a bilayer membrane are assumed to slide freely with respect to each other. The lipid of a single monolayer is modeled as an effective flexible string with a given incompressible area, A_n, and finite bending rigidity, K_f (see Fig. 1), subjected to the confining parabolic potential. The latter allows for a repulsive entropic force induced between the neighboring lipid molecules in the same monolayer, due to excluded volume effect (see Fig. 2). Interaction between heads is effectively included into surface tension in the hydrophobic region. Energy functional of the string consists of kinetic energy and bending energy of a given dynamical string conformation, as well as potential energy in the confining potential induced by collisions with the neighboring strings:

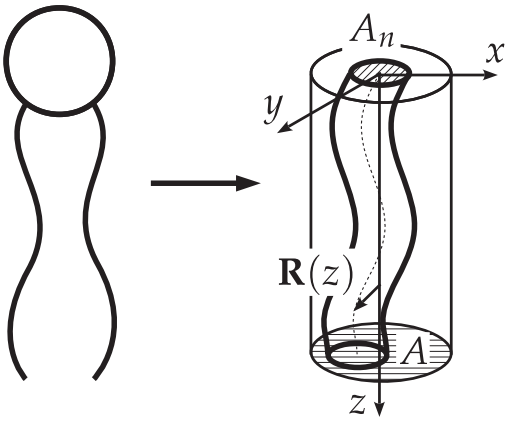

FIG. 1. Hydrocarbon tails of lipid are modeled as a flexible string. Schematic representations.

$$E_t = \int_0^L \left[\frac{\rho \dot{\mathbf{R}}^2}{2} + \frac{K_f}{2} \left(\frac{\partial^2 \mathbf{R}}{\partial z^2} \right)^2 + \frac{B\mathbf{R}^2}{2} \right] \mathrm{d}z. \qquad (2)$$

Here, ρ is a string linear density, $\mathbf{R}(z) = \{R_x(z), R_y(z)\}$ is a vector in the plane of the membrane giving the deviation of a string from the straight line as a function of the coordinate along the axis normal to the membrane plane (see Fig. 1), and B is a parameter of the confining potential determined self-consistently. A self-consistent parabolic potential has been used previously to model a polymer chain in confined geometry [37]. That approach is conceptually close to the statistical kink-model [38,39], which was used to find the probability distribution function of chain conformations and macroscopic membrane characteristics, minimizing the free energy of the membrane. In contrast to that model we use a continuous description of the lipid chain bending fluctuation and include an option of the direct self-assembly of lipids in membrane.

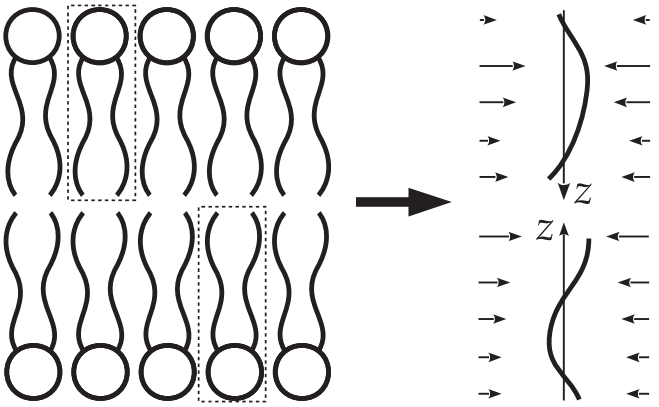

FIG. 2. Collisions with neighboring lipids are modeled by self-consistent confining potential. Potential is parabolic in the string deviation from axis z (arrows size mimics local force strength).

Boundary conditions for the model flexible string take into account the following physical assumptions [the same is assumed also for component $R_y(z)$]:

$$\begin{aligned} R_x'(0) &= 0 && \text{a chain terminates perpendicularly to the membrane surface,} \\ R_x'''(0) &= 0 && \text{net force acting on a head is zero,} \\ R_x''(L) &= 0 && \text{net torque acting at a chain's free end is zero,} \\ R_x'''(L) &= 0 && \text{net force acting at a chain free end is zero.} \end{aligned} \quad (3)$$

The first boundary condition reflects the orientational asymmetry of the monolayer due to water-lipid interface which is clearly seen from data on the molecules orientational order parameter [40,41]: lipid tails are more ordered in the vicinity of head groups constrained by the hydrophobic tension. Yet, the chains are not permanently perpendicular to the membrane surface, and boundary conditions are approximate and necessary to keep the model analytically solvable.

Assuming the membrane to be locally isotropic in the lateral plane, the partition function can be split in the product of the two equal components, $Z = Z_x Z_y = Z_x^2$, and thus the free energy of the lateral oscillations of the chain equals to

$$F_t = -2k_BT \log Z_x. \quad (4)$$

The partition function Z_x could be written as a path integral over all chain conformations:

$$Z_x = \iint \mathrm{e}^{-\frac{E\{R_x(z),\dot{R}_x(z)\}}{k_BT}} \mathrm{D}R_x \mathrm{D}\dot{R}_x \quad (5)$$

Under the boundary conditions Eq. (3) potential part of the energy functional Eq. (2) can be equivalently rewritten in terms of linear Hermitian operator $\hat{H} = B + K_f \frac{\partial}{\partial z^4}$ in the form

$$E_{t(\mathrm{pot})} = \sum_{\alpha=x,y} E_\alpha, \quad E_\alpha \equiv \int_0^L [R_\alpha(z)\hat{H}R_\alpha(z)]\,\mathrm{d}z. \quad (6)$$

Then, an arbitrary conformation of the chain is expressed as the deviation of the centers of the string, $R_{x,y}(z)$, from the straight vertical line (see Fig. 1), and is parametrized by an infinite set of coefficients C_n of the linear decomposition of the function $R_{x,y}(z)$ over the eigenfunctions $R_n(z)$ of the operator $\hat{H}$:

$$R_{\alpha=x,y}(z) = \sum_n C_{n,\alpha} R_n(z), \quad \hat{H}R_n(z) = E_n R_n(z). \quad (7)$$

Substituting Eq. (7) into Eq. (2) and using the standard orthogonality property of the eigenfunctions of operator $\hat{H}$, enables a simple decomposition of the energy functional into the series

$$E_t = \sum_n \frac{1}{2}\{\rho\dot{C}_n^2 + E_n C_n^2\}. \quad (8)$$

We thus see that energy of a fluctuating string in a parabolic potential maps on the sum of energies of harmonic oscillators with rigidities E_n. Hence, the Boltzmann's probability of the state of a string in an arbitrary conformation $R_{x,y}(z)$, $P(\{R_{x,y}(z)\})$, is proportional to the infinite product of the Boltzmann's probabilities of the states of these oscillators due to the obvious relation

$$P(\{R_{x,y}(z)\}) \propto \exp\left\{-\frac{E_t}{k_BT}\right\} \sim \prod_n \exp\left\{-\frac{\epsilon_n}{k_BT}\right\},$$
$$\epsilon_n \equiv \frac{1}{2}\{\rho\dot{C}_n^2 + E_n C_n^2\}. \quad (9)$$

Therefore, the distribution of the coefficients C_n prove to be just Gaussian Boltzmann's distribution, which makes the whole thermodynamic theory of the lipid membrane analytically tractable. The corresponding eigenvalues E_n and eigenfunctions $R_n(z)$ of the operator $\hat{H} = B + K_f \frac{\partial}{\partial z^4}$ are [35]

$$n = 0 \Rightarrow \begin{cases} E_0 = B \\ R_0(z) = \sqrt{1/L}, \end{cases}$$
$$n \in \mathbb{N} \Rightarrow \begin{cases} c_n = \pi n - \frac{\pi}{4} \\ E_n = B + c_n^4 \frac{K_f}{L^4} \\ R_n(z) = \sqrt{\frac{2}{L}}\left[\cos\left(c_n \frac{z}{L}\right) + \frac{\cos(c_n)}{\cosh(c_n)}\cosh\left(c_n \frac{z}{L}\right)\right] \end{cases}. \quad (10)$$

This gives the following product of the Gaussian integrals for the partition function:

$$Z_x = \int_{-\infty}^{+\infty} \prod_n \mathrm{e}^{-\frac{(\rho\dot{C}_n)^2}{2\rho k_BT} - \frac{C_n^2 E_n}{2k_BT}} \frac{\mathrm{d}(\rho\dot{C}_n)\cdot \mathrm{d}C_n}{2\pi\hbar} = \prod_n \frac{k_BT}{\hbar}\sqrt{\frac{\rho}{E_n}}. \quad (11)$$

To derive the dependence of the monolayer thickness, L, on the temperature we relate it to the contour length of the lipid chain L_R proportional to the number of CH_2 groups in the lipid tail:

$$L_R = \int_0^L \sqrt{1 + \left\langle\left(\frac{\partial\vec{R}}{\partial z}\right)^2\right\rangle}\,\mathrm{d}z. \quad (12)$$

Expanding this finally yields the equation for L which might be solved numerically:

$$L_R = L + \frac{2k_BTL^2}{K_f} \times \sum_{n=1} \frac{c_n^2 \int_0^1 \left(\sin(c_n x) - \frac{\cos c_n}{\cosh c_n}\sinh(c_n x)\right)^2 \mathrm{d}x}{B + c_n^4 \frac{K_f}{L^4}} \quad (13)$$

(for derivation see Appendix A).

To derive the self-consistency equation for so far unknown parameter B, we differentiate both sides of Eq. (4) with respect to B and readily obtain the self-consistency equation for this parameter:

$$\frac{\partial F_t}{\partial B} = L\langle R_x^2\rangle, \quad (14)$$

where brackets denote the thermodynamic (Boltzmann) average over chain conformations. The right-hand side of Eq. (14) is directly expressed via the thermodynamic average area per lipid A in the membrane plane and effective incompressible area of lipid chain A_n:

$$\pi\langle R_x^2 + R_y^2\rangle = 2\pi\langle R_x^2\rangle = (\sqrt{A} - \sqrt{A_n})^2. \quad (15)$$

Here, an isotropy of the membrane in the x, y plane is assumed for simplicity. Using this relation one can rewrite

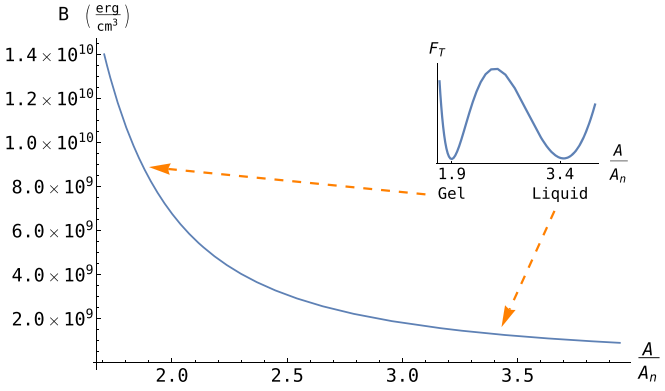

FIG. 3. Entropic repulsion stiffness B at the phase transition changes by an order of magnitude: in gel phase area per lipid $A/A_n \approx 1.9$, $B \approx 9\times10^9$ erg/cm^3, whereas in liquid phase $A/A_n \approx 3.4$, $B \approx 1\times10^9$ erg/cm^3. DPPC lipid bilayer is used as a reference. The choice of the microscopic model parameters: $L_R = 17$ Å, $A_n = 20$ Å^2, $K_f = 5.797\times10^{-21}$ erg cm, and $U = 745$ kcal Å^6/mol, are made to match respective DPPC micro- and macroscopic parameters, such as main transition temperature and area per lipid in the vicinity of the transition.

Eq. (14) in the explicit form exploiting Eq. (11):

$$\sum_{n=0} \frac{1}{B\frac{L^4}{K_f} + c_n^4} = \frac{K_f A_n}{\pi k_B T L^3}\left(\sqrt{\frac{A}{A_n}} - 1\right)^2. \tag{16}$$

Solving this equation one finds $B(A)$.

Now, like in our recent work [42], we add van der Waals attraction energy between the lipid chains to the free energy of the string, which now contains as well the sum of the lipid tail free energy Eq. (10) and hydrophobic tension energy γA:

$$\frac{F_T}{k_B T} = \frac{F_t(A)}{k_B T} + \frac{\gamma A}{k_B T} - \frac{9\pi^{7/2}}{2^8}\frac{UN^2}{LA^{5/2}k_B T} \tag{17}$$

One obtains the area per lipid in a membrane by minimizing free energy Eq. (17). In the previous work [42] this led us to a description of the liquid-gel phase transition. Here, it is important to mention that solving the self-consistency equation (16) we obtain, besides the abrupt change of the area per lipid, also a jump in the magnitude of the stiffness B of the entropic repulsion potential acting on the lipid chain in the membrane at the liquid-gel transition, see Fig. 3. Thus, we have found a physical phenomenon, that constitutes an abrupt change in the stiffness B of entropic repulsion between fluctuating flexible lipid chains at the main phase transition. In the next section we calculate the consequences of this behavior for the temperature dependence of the lipids lateral self-diffusion coefficient.

III. THE LIPIDS LATERAL SELF-DIFFUSION COEFFICIENT

In terms of semi-flexible strings model, A_n of Eq. (1) might be interpreted as the incompressible area of the string.

$D(A_v)$ is considered to be slowly varying function of void size, A_v, and is estimated as $D(A_v) \sim l\upsilon$ [29], where υ is characteristic lateral velocity of the lipid molecule inside the cage, and l is mean free path given by the cage diameter. υ has been measured in [43], and was found to be $\upsilon_0 = 1.12$ m/s in the DMPC liquid-crystalline phase. Estimating l as a void diameter one arrives at

$$D(A_n) = \upsilon_0 \cdot 2\sqrt{\frac{A_n}{\pi}}. \tag{18}$$

The $P(A_v)$ and $P(E)$ distribution functions are defined as follows [34]:

$$P(A_v) = \frac{\exp\left(-\frac{A_v}{A-A_n}\right)}{\int_{A_n}^{\infty}\exp\left(-\frac{A_v}{A-A_n}\right)\mathrm{d}A_v},$$
$$P(E) = \frac{E}{(k_B T)^2}\exp\left(-\frac{E}{k_B T}\right). \tag{19}$$

The expression for $P(E)$ is the Boltzmann's statistics distribution function for two-dimensional classic oscillators [44] (see Appendix B). So that $P(A_v)P(E)\,\mathrm{d}A_v\,\mathrm{d}E$ is the probability that the lipid possesses energy in the interval E and $E + \mathrm{d}E$ and there is an adjacent void of area, originated by dynamical defects, in the range of A_v and $A_v + \mathrm{d}A_v$. Substitution of Eq. (19) into Eq. (1) leads to

$$D = D(A_n)\left(1 + \frac{E_a}{k_B T}\right)\exp\left(-\frac{A_n}{A - A_n} - \frac{E_a}{k_B T}\right). \tag{20}$$

Whereas activation energy E_a might be estimated as an average entropic repulsion energy given by the third term in Eq. (2):

$$E_a = \frac{B\langle R^2\rangle L}{2} \equiv \frac{B(\sqrt{A} - \sqrt{A_n})^2 L}{2\pi}. \tag{21}$$

The results of the calculation of the temperature dependence of the diffusion coefficient expressed by Eqs. (20) and (21) are plotted in Fig. 4.

The self-diffusion coefficient in DPPC measured at the nanosecond timescale above and below main transition temperature has been reported in [45]. Those authors found the self-diffusion coefficient to be $D = (4 \pm 1)\times10^{-6}$ cm^2/s at 336 K, and 1.4×10^{-7} cm^2/s at 306 K (see Fig. 4).

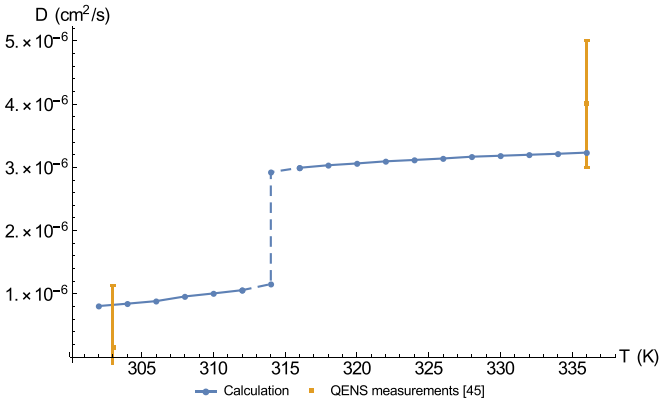

FIG. 4. Calculation results of self-diffusion coefficient for the DPPC in rattling in a cage mode obtained using hybrid equation (20). Our approach is limited to homogeneous phases, hence, in the vicinity of the phase transition calculation is shown with dashes. Two points with error bars are QENS measurements [45].

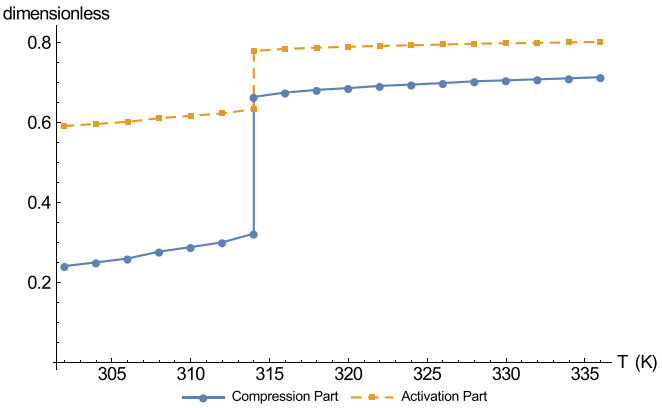

FIG. 5. "Compression" (solid) and "activation" (dashed) factors of the self-diffusion coefficient [see Eq. (22)].

To understand the drop in the self-diffusion coefficient let us split the self-diffusion coefficient into two factors, "compression" and "activation":

$$D = D(A_n)\underbrace{\exp\left(-\frac{A_n}{A-A_n}\right)}_{\text{compression}}\cdot\underbrace{\left(1+\frac{E_a}{k_BT}\right)\exp\left(-\frac{E_a}{k_BT}\right)}_{\text{activation}}. \tag{22}$$

Plotting the change of these factors with temperature following from Fig. 3, one sees that "compression" gives a major contribution to the drop of the self-diffusion coefficient (see Fig. 5). This is obvious from the fact that at the phase transition the "compression" part changes by two times, whereas the "activation" part changes only by about 20%. Still, without the "activation" contribution the curve in Fig. 4 shifts up, and does not match experimental data at lower temperatures. Hence, both contributions are required to get a more faithful description of the diffusion coefficient temperature dependence.

The "compression" factor's drop reflects the smaller available area for the lipid jumps in the gel phase as compared with the liquid phase. The "activation" factor has entropic nature: it is related to the stiffness, B, of the mean-field confining potential [see Eqs. (21) and (7)], which reflects the strength of entropic repulsion in the membrane. Liquid-gel phase transition leads to twofold change in area per lipid, which, according to Eq. (16), yields an order of magnitude change in entropic repulsion stiffness.

Indeed, the inset in Fig. 3 shows the free energy of the lipid, Eq. (17), at the main phase transition temperature, T_c. The two minima of the inset are the areas per lipid in gel and liquid phases at Tc. Figure 3 plots $B(A)$ dependency defined by the self-consistency equation (16). Substituting areas per lipid of gel and liquid phases, one sees an order of magnitude change in entropic repulsion stiffness.

IV. DISCUSSION

The problem of the variation of the lipids diffusion coefficient across the main phase transition was lacking a theoretical description so far. The complexity of this phenomenon reveals itself in the existence of the two time scales with different qualitative mechanisms of the lateral lipid diffusion. A diffusion process on the time scale greater than hundreds of nanoseconds constitutes cooperative fluctuations of large molecular clusters. On the other hand, a single molecule rattling in cage processes are responsible for the lateral diffusion on the shorter time scale, and our model is relevant for this regime.

We should note that we use equilibrium thermodynamics, neglecting fluctuations and collective phenomena, which yield the abrupt jump in monolayer characteristics. More detailed considerations would smear the jump and lead to a continuous change in the diffusion coefficient. For this reason the value of the self-diffusion coefficient is shown in dashes in the vicinity of the phase transition in Fig. 4.

The self-diffusion coefficient is the product of "activation" and "compression" factors. The later is a direct consequence of area per lipid change at the phase transition, whereas the former is due to a change in entropic repulsion stiffness.

In conclusion, we have found that the stiffness of entropic repulsion between the fluctuating lipid chains, and area per lipid may abruptly change at the liquid-gel phase transition. This change causes, in turn, the drop of the lipids lateral self-diffusion coefficient in the membranes on the short time scale. In general, lipid lateral self-diffusion in the lipid membranes is a complex phenomenon with two time scales differing by underlying physical processes. Lipid self-diffusion is a collective process on the time scale of hundreds of nanoseconds, whereas at shorter times the diffusion constitutes individual lipids jumps. The last regime fits single-molecule mean-field theories and a free-volume theory of diffusion. We applied flexible strings mean-field theory of the lipid membrane to a free-volume theory augmented with an activation factor in the expression for the diffusion coefficient. The self-diffusion coefficient is composed of "activation" and "compression" factors. The latter is a direct consequence of area per lipid change at the phase transition, whereas the former is due to an order of magnitude change in entropic repulsion.

ACKNOWLEDGMENTS

The authors gratefully acknowledge the financial support of this work by Russian Science Foundation grant (Project No. 17-79-20440) and by the Government of Russian Federation through Goszadanie research project Grant No. 11.8411.2017.

APPENDIX A: DERIVATION OF CHAIN'S CONSTANT CONTOUR LENGTH CONDITION

Assuming the chain's full (contour) length, L_R, is constant one has

$$L_R = \int_0^L \sqrt{1+\left\langle\left(\frac{\partial\vec{R}}{\partial z}\right)^2\right\rangle}\,\mathrm{d}z. \tag{A1}$$

Our goal here is to express the chain's length in terms of full length and other properties of the string. To that end we evaluate the integral in Eq. (A1).

One can rewrite the mean value under the square root

$$\begin{aligned}\vec{R} &= R_x\vec{e}_x + R_y\vec{e}_y,\\ \frac{\partial\vec{R}}{\partial z} &= \frac{\partial R_x}{\partial z}\vec{e}_x + \frac{\partial R_y}{\partial z}\vec{e}_y,\\ \left(\frac{\partial\vec{R}}{\partial z}\right)^2 &= \left(\frac{\partial R_x}{\partial z}\right)^2 + \left(\frac{\partial R_y}{\partial z}\right)^2,\\ \left\langle\left(\frac{\partial\vec{R}}{\partial z}\right)^2\right\rangle &= \left\langle\left(\frac{\partial R_x}{\partial z}\right)^2\right\rangle + \left\langle\left(\frac{\partial R_y}{\partial z}\right)^2\right\rangle\\ &\equiv 2\left\langle\left(\frac{\partial R_x}{\partial z}\right)^2\right\rangle. \end{aligned} \tag{A2}$$

Substituting Eq. (A2) into Eq. (A1) leads to

$$\begin{aligned}L_R &= \int_0^L \sqrt{1+2\left\langle\left(\frac{\partial R_x}{\partial z}\right)^2\right\rangle}\,\mathrm{d}z\\ &\approx \int_0^L \left(1+\left\langle\left(\frac{\partial R_x}{\partial z}\right)^2\right\rangle\right)\mathrm{d}z\\ &= L + \int_0^L \left\langle\left(\frac{\partial R_x}{\partial z}\right)^2\right\rangle\mathrm{d}z. \end{aligned} \tag{A3}$$

The mean value under the integral is evaluated using the following relations:

$$\begin{aligned}R_x &= \sum_n C_n R_n,\\ R'_x &= \sum_n C_n R'_n,\\ (R'_x)^2 &= \sum_{n,m} C_n C_m R'_n R'_m,\\ \langle(R'_x)^2\rangle &= \sum_{n,m}\langle C_n C_m\rangle R'_n R'_m = \sum_n \frac{k_B T}{E_n}(R'_n)^2. \end{aligned} \tag{A4}$$

Upon calculating R'_n [see Eq. (10) in the main text], substituting Eq. (A4) into Eq. (A3) and introducing the dimensionless coordinate $x = z/L$, one arrives at the equation for L:

$$L_R = L + \frac{2k_B T L^2}{K_f}\sum_{n=1}\frac{c_n^2\int_0^1 (r'_n)^2\,\mathrm{d}x}{B + c_n^4\frac{K_f}{L^4}}, \tag{A5}$$

which is Eq. (13) in the main text.

APPENDIX B: PROBABILITY DENSITY OF CLASSICAL HARMONIC OSCILLATOR WITH THE GIVEN ENERGY

For simplicity, let us continue with the 1D case. Consider N classical oscillators at temperature T. The number distribution of oscillators with generalized coordinates x and p_x is given by

$$n(x,\,p_x) = \frac{N\exp\left(\frac{-E(x,p_x)}{k_B T}\right)}{\iint\exp\left(\frac{-E(x,p_x)}{k_B T}\right)\mathrm{d}x\,\mathrm{d}p_x}. \tag{B1}$$

Energy of the harmonic oscillator is given by

$$E = \frac{p_x^2}{2m} + \frac{1}{2}m(2\pi\nu)^2 x^2. \tag{B2}$$

Dividing both parts of Eq. (B2) by E transforms Eq. (B2) into an equation of ellipse with the area

$$V_2 = \pi\left(\frac{E}{\pi\nu}\right) \equiv \frac{E}{\nu}. \tag{B3}$$

In the quasi-classical limit,

$$E = h\nu\cdot n, \tag{B4}$$

hence

$$V_2 = hn \quad\Rightarrow\quad \delta V_2 = h\cdot\delta n. \tag{B5}$$

On the other hand, $\delta V_2 = \mathrm{d}x\,\mathrm{d}p_x$, which leads to

$$\mathrm{d}x\,\mathrm{d}p_x = h\,\mathrm{d}n. \tag{B6}$$

Using Eqs. (B4) and (B6) we are now in a position to calculate the number of oscillators with generalized coordinates x and p_x, Eq. (B1), that proves to be

$$n(x,\,p_x) = \frac{\nu}{k_B T}N\exp\left(\frac{-E(x,\,p_x)}{k_B T}\right). \tag{B7}$$

Now consider the number of oscillators with energy in the interval from E to $E+\mathrm{d}E$:

$$\begin{aligned} n(E)\,\mathrm{d}E &= n(x,\,p_x)\cdot\mathrm{d}V_2\\ \Rightarrow\; n(E)\,\mathrm{d}E &= \frac{\nu}{k_B T}N\exp\left(-\frac{E}{k_B T}\right)\frac{\delta E}{\nu}, \end{aligned} \tag{B8}$$

which leads to the expression for the probability density of the number of classical oscillators with energy E:

$$P_{1D}(E) \equiv \frac{n(E)}{N} = \frac{1}{k_B T}\exp\left(-\frac{E}{k_B T}\right). \tag{B9}$$

In the 2D case one would have

$$V_4 = \frac{\pi^2}{2}\left(\frac{E}{\pi\nu}\right)^2 \equiv \frac{1}{2}\frac{E^2}{\nu^2} \tag{B10}$$

in place of Eq. (B3), which leads to

$$\begin{aligned} V_4 &= \frac{h^2 n^2}{2},\\ \delta V_4 &= h^2 n\delta n \equiv \mathrm{d}x\mathrm{d}p_x\cdot\mathrm{d}y\mathrm{d}p_y, \end{aligned} \tag{B11}$$

in the quasi-classical limit. The 2D analog of Eq. (B7) is then

$$\begin{aligned} &n(x,\,p_x,\,y,\,p_x)\\ &= \frac{N\exp\left(\frac{-E(x,p_x)-E(y,p_y)}{k_B T}\right)}{\iiint\exp\left(\frac{-E(x,p_x)-E(y,p_y)}{k_B T}\right)\mathrm{d}x\,\mathrm{d}p_x\,\mathrm{d}y\,\mathrm{d}p_y}\\ &= \frac{N\exp\left(\frac{-E}{k_B T}\right)}{\iint\exp\left(\frac{-E(x,p_x)}{k_B T}\right)\mathrm{d}x\,\mathrm{d}p_x\iint\exp\left(\frac{-E(y,p_y)}{k_B T}\right)\mathrm{d}y\,\mathrm{d}p_y}\\ &= \left(\frac{\nu}{k_B T}\right)^2 N\exp\left(-\frac{E}{k_B T}\right), \end{aligned}$$

which leads to the analog of Eq. (B8):

$$n(E)\,\mathrm{d}E = \left(\frac{\nu}{k_B T}\right)^2 N \exp\left(-\frac{E}{k_B T}\right) \cdot \frac{E\delta E}{\nu^2}, \qquad \text{(B12)}$$

which, in turn, leads to the second relation in Eq. (19) of the main text.

[1] S. J. Singer and G. L. Nicolson, Science **175**, 720 (1972).
[2] F. M. Goñi, Biochim. Biophys. Acta (BBA) - Biomem. **1838**, 1467 (2014).
[3] V. S. Markin and B. Martinac, Biophys. J. **60**, 1120 (1991).
[4] S. Sukharev, S. R. Durell, and H. R. Guy, Biophys. J. **81**, 917 (2001).
[5] K. Simons and E. Ikonen, Nature **387**, 569 (1997).
[6] B. Alberts, A. Johnson, J. Lewis, M. Raff, K. Roberts, and P. Walter, *Molecular Biology of the Cell*, 5th ed. (Garland Science, New York, 2007).
[7] G. van Meer, D. R. Voelker, and G. W. Feigenson, Nat. Rev. Mol. Cell Biol. **9**, 112 (2008).
[8] C.-h. Huang and S. Li, Biochim. Biophys. Acta (BBA) - Rev. Biomem. **1422**, 273 (1999).
[9] M. J. Janiak, D. M. Small, and G. G. Shipley, J. Biol. Chem. **254**, 6068 (1979).
[10] K. Akabori and J. F. Nagle, Soft Matter **11**, 918 (2015).
[11] S.-S. Qin, Z.-W. Yu, and Y.-X. Yu, J. Phys. Chem. B **113**, 8114 (2009).
[12] S. W. Chiu, E. Jakobsson, R. J. Mashl, and H. L. Scott, Biophys. J. **83**, 1842 (2002).
[13] D. A. Brown and E. London, J. Biol. Chem. **275**, 17221 (2000).
[14] M. Fuhrmans and S. J. Marrink, J. Am. Chem. Soc. **134**, 1543 (2012).
[15] H. T. McMahon, M. M. Kozlov, and S. Martens, Cell **140**, 601 (2010).
[16] V. A. Frolov, A. Escalada, S. A. Akimov, and A. V. Shnyrova, Chem. Phys. Lip. **185**, 129 (2014).
[17] A. V. Shnyrova, P. V. Bashkirov, S. A. Akimov, T. J. Pucadyil, J. Zimmerberg, S. L. Schmid, and V. A. Frolov, Science **339**, 1433 (2013).
[18] B. S. Lee, S. A. Mabry, A. Jonas, and J. Jonas, Chem. Phys. Lipids **78**, 103 (1995).
[19] V. K. Sharma, E. Mamontov, D. B. Anunciado, H. O'Neill, and V. Urban, J. Phys. Chem. B **119**, 4460 (2015).
[20] P. Almeida and W. Vaz, in *Structure and Dynamics of Membranes*, edited by R. Lipowsky and E. Sackmann (Elsevier, New York, 1995).
[21] J. Wohlert and O. Edholm, J. Chem. Phys. **125**, 204703 (2006).
[22] E. Flenner, J. Das, M. C. Rheinstädter, and I. Kosztin, Phys. Rev. E **79**, 011907 (2009).
[23] W. Pfeiffer, T. Henkel, E. Sackmann, W. Knoll, and D. Richter, Europhys. Lett. **8**, 201 (1989).
[24] S. Känig, T. M. Bayerl, G. Coddens, D. Richter, and E. Sackmann, Biophys. J. **68**, 1871 (1995).
[25] M. C. Rheinstädter, C. Ollinger, G. Fragneto, F. Demmel, and T. Salditt, Phys. Rev. Lett. **93**, 108107 (2004).
[26] S. H. Chen, C. Y. Liao, H. W. Huang, T. M. Weiss, M. C. Bellisent-Funel, and F. Sette, Phys. Rev. Lett. **86**, 740 (2001).
[27] E. Wu, K. Jacobson, and D. Papahadjopoulos, Biochemistry **16**, 3936 (1977).
[28] W. L. Vaz and P. F. Almeida, Biophys. J. **60**, 1553 (1991).
[29] M. H. Cohen and D. Turnbull, J. Chem. Phys. **31**, 1164 (1959).
[30] M. C. Rheinstädter, J. Das, E. J. Flenner, B. Brüning, T. Seydel, and I. Kosztin, Phys. Rev. Lett. **101**, 248106 (2008).
[31] E. Falck, T. Róg, M. Karttunen, and I. Vattulainen, J. Am. Chem. Soc. **130**, 44 (2008).
[32] U. Wanderlingh, G. D'Angelo, C. Branca, V. Conti Nibali, A. Trimarchi, S. Rifici, D. Finocchiaro, C. Crupi, J. Ollivier, and H. D. Middendorf, J. Chem. Phys. **140**, 174901 (2014).
[33] S. Block, Biomolecules **8**, 30 (2018).
[34] H. S. Chung, J. Chem. Phys. **44**, 1362 (1966).
[35] S. I. Mukhin and S. Baoukina, Phys. Rev. E **71**, 061918 (2005).
[36] S. I. Mukhin and B. B. Kheyfets, Phys. Rev. E **82**, 051901 (2010).
[37] T. W. Burkhardt, J. Phys. A: Math. Gen. **28**, L629 (1995).
[38] I. Szleifer, D. Kramer, A. Ben-Shaul, D. Roux, and W. M. Gelbart, Phys. Rev. Lett. **60**, 1966 (1988).
[39] I. Szleifer, D. Kramer, A. Ben-Shaul, W. M. Gelbart, and S. A. Safran, J. Chem. Phys. **92**, 6800 (1990).
[40] E. Lindahl and O. Edholm, Biophys. J. **79**, 426 (2000).
[41] L. S. Vermeer, B. L. de Groot, V. Réat, A. Milon, and J. Czaplicki, Eur. Biophys. J. **36**, 919 (2007).
[42] B. Kheyfets, T. Galimzyanov, and S. Mukhin, JETP Lett. **107**, 718 (2018).
[43] C. L. Armstrong, M. Trapp, J. Peters, T. Seydel, and M. C. Rheinstädter, Soft Matter **7**, 8358 (2011).
[44] G. S. Rushbrooke, *Introduction to Statistical Mechanics*, reprint edition (Clarendon Press, Oxford, 1949).
[45] J. Tabony and B. Perly, Biochim. Biophys. Acta **1063**, 67 (1991).